arTs Università degli Studi di Trieste
Archivio della ricerca – postprint

Critical water contents at leaf, stem and root level leading to irreversible drought-induced damage in two woody and one herbaceous species

Patrizia Trifilò[1] | Elisa Abate[1] | Francesco Petruzzellis[2] | Maria Azzarà[1] | Andrea Nardini[2]

[1]Dipartimento di Scienze Chimiche, Biologiche, Farmaceutiche ed Ambientali, Università di Messina, Messina, Italy

[2]Dipartimento di Scienze della Vita, Università di Trieste, Trieste, Italy

Correspondence
Patrizia Trifilò, Dipartimento di Scienze Chimiche, Biologiche, Farmaceutiche ed Ambientali, Università di Messina, salita F. Stagno D'Alcontres 31, 98166 Messina, Italy.
Email: ptrifilo@unime.it

Funding information
FFABR Unime

Abstract

Plant water content is a simple and promising parameter for monitoring drought-driven plant mortality risk. However, critical water content thresholds leading to cell damage and plant failure are still unknown. Moreover, it is unclear whether whole-plant or a specific organ water content is the most reliable indicator of mortality risk. We assessed differences in dehydration thresholds in leaf, stem and root samples, hampering the organ-specific rehydration capacity and increasing the mortality risk. We also tested eventual differences between a fast experimental dehydration of uprooted plants, compared to long-term water stress induced by withholding irrigation in potted plants. We investigated three species with different growth forms and leaf habits i.e., *Helianthus annuus* (herbaceous), *Populus nigra* (deciduous tree) and *Quercus ilex* (evergreen tree). Results obtained by the two dehydration treatments largely overlapped, thus validating bench dehydration as a fast but reliable method to assess species-specific critical water content thresholds. Regardless of the organ considered, a relative water content value of 60% induced significant cell membrane damage and loss of rehydration capacity, thus leading to irreversible plant failure and death.

KEYWORDS
cell rehydration capacity, drought, gas exchange, membrane damage, mortality risk, water content

1 | INTRODUCTION

Increasing frequency and intensity of drought events is a very likely consequence of climate warming (IPCC, 2013; Pokhrel et al., 2021). Anomalous drought and heat waves have already produced severe damage to forests and crops, including reduction in productivity, plant decline and death (i.e., Allen et al., 2010; Goulart et al., 2021; Hartmann et al., 2018; Klein & Hartmann, 2018; Lesk et al., 2016). Ecological and economical effects of these phenomena have prompted interest into the understanding of processes underlying drought-driven plant death (i.e., Allen et al., 2015; Choat et al., 2018; McDowell et al., 2008, 2019), and the identification of simple and reliable proxies of actual risk of forests and crops failure during drought events.

Previous studies have highlighted the key role of hydraulic functioning for plant resistance and resilience to water stress (Nardini et al., 2018). In particular, the blockage of the long-distance water transport system (i.e., hydraulic failure) is recognised as one of the major drivers of drought-induced plant mortality. In fact, soil dehydration can induce the failure of the root-to-soil contact, leading to stomatal closure but hampering water uptake (Abdalla et al., 2021; Carminati & Javaux, 2020). Progressive plant dehydration due to

residual water loss from leaves and bark causes xylem water potential to decrease, leading to xylem embolism spread and further reducing water supply to plant cells and tissues (Choat et al., 2018). Several studies have tried to identify critical levels of embolism-induced loss of hydraulic conductance leading to irreversible plant failure, and it is generally agreed that these values set between 50% and 90% (Arend et al., 2021; Barigah et al., 2013; Hammond et al., 2019; Urli et al., 2013). Because hydraulic failure is frequently associated with irreversible plant decline, embolism levels in field-growing plants are a good indicator of species- and individual-risk of death under drought (Davis et al., 2002; Nardini et al., 2013). However, field measurements of percentage loss of hydraulic conductance (PLC) at large spatial and temporal scales are not feasible with current techniques, making it difficult to use this physiological proxy to monitor the risk of irreversible plant failure.

Despite the importance of hydraulic failure in the processes leading to plant decline, it should be remembered that ultimately, plant death is triggered by critical dehydration levels inducing reactive oxygen species accumulation, membrane disruption, and meristem death, hampering the plant ability to recover after drought (Abate et al., 2021; Mantova et al., 2021, 2022). Hence, measurements of the relative water content (RWC) have been proposed as a possible tool for monitoring the risk of drought-induced plant failure (Martinez-Vilalta et al., 2019), also considering that canopy water content can be estimated over large spatial and temporal scales by remote sensing techniques (i.e., Marusig et al., 2020; Nardini et al., 2021; Rao et al., 2019; Saatchi et al., 2013). Robust correlations have been recorded between RWC and embolism rate (Abate et al., 2021; Mantova et al., 2021; Rosner et al., 2019; Trueba et al., 2019), nonstructural carbohydrates content (Sapes & Sala, 2021; Sapes et al., 2019), loss of rehydration capacity, relative electrolyte leakage (REL) (a proxy of cell membrane damage), and leaf water transport efficiency (Abate et al., 2021; Guadagno et al., 2017; Trifilò et al., 2021; Trueba et al., 2019). Overall, these results strongly encourage the use of cell, tissue and organ water content as reliable and easier to measure proxies of plant health compared to PLC.

However, the reliability of water content measurements as predictors of mortality risk still needs to be investigated in depth. In particular, it is still unclear if whole plant or a specific organ water content threshold is the most reliable indicator of mortality risk. Rosner et al. (2019) have reported good correlations between stem RWC and the loss of hydraulic conductivity in some tree species. In this light, RWC and hydraulic conductivity losses are two linked processes. On the other hand, RWC appeared useful for predicting the loss of hydraulic conductivity in woody angiosperms but not in conifers (Mantova et al., 2021). This result may be explained by the differences in wood density and, then, wood capacitance values that typically occur in angiosperm versus gymnosperm species (i.e., Kiorapostolou et al., 2019). In fact, higher wood capacitance values affect the dehydration time. Therefore, there may be discrepancies in the link between PLC and RWC values, when comparing groups with different capacitance values.

There is general consensus that leaf hydraulic vulnerability is a major driver of plant hydraulics under drought (Brodribb & Holbrook, 2004; Brodribb et al., 2005; Hochberg et al., 2017; Scoffoni et al., 2016; Skelton et al., 2017; Trifilò et al., 2003; Wang et al., 2018; Xiong & Nadal, 2020). Therefore, it is plausible to hypothesise that leaf water content might be a reliable proxy of risk of plant death. Finally, the critical percentage RWC threshold leading to plant failure is still not clearly quantified, and it is not known whether this is similar or not in different species and organs. Surprisingly, measurements of mortality risk as a function of leaf, stem, root and whole plant water content are still relatively rare in the literature (Kursar et al., 2009; Sapes & Sala, 2021; Sapes et al., 2019; Tyree et al., 2002). It has been demonstrated that the decline in water status, commonly estimated in terms of decline of leaf water potential, has an impact on gas exchange, reducing carbon gain and potentially leading to carbon starvation (i.e., Klein, 2014; McDowell et al., 2022; Trifilò et al., 2017). For the same reason, drought-driven decrease in RWC (a parameter that summarises symplastic and apoplastic water content), is expected to be coupled to stomatal closure. In this light, correlations may exist between critical RWC values and stomatal closure. As an additional note, there is no information on the best methodological procedures to identify critical water content values, with specific reference to whole plant dehydration over mid- to long time scales, compared to fast bench dehydration of detached plant organs or uprooted plants.

In the present study, we report measurements of dehydration-induced changes in RWC, membrane damage and loss of rehydration capacity at leaf, stem, root and whole plant levels. We specifically investigated: (i) the eventual differences between a fast experimental dehydration, compared to long-term water stress; (ii) the possible differences in lethal RWC thresholds among leaf, stem and root samples, and their correlation with organ-specific rehydration capacity, membrane damage, and plant mortality; (iii) the relationships between stomatal behaviour and organ dehydration. We expected that critical RWC values would induce (or be coordinated with) stomatal closure to limit further water loss and eventual cell damage. To test for the general applicability of this approach to different plant types, we focused our analysis on three species encompassing different growth forms and leaf habits: *Helianthus annuus* L. (an herbaceous species), *Populus nigra* L. (a deciduous tree) and *Quercus ilex* L. (an evergreen tree).

2 | MATERIALS AND METHODS

2.1 | Plant material and experimental planning

Experiments were performed in summer 2020 on 1-year-old saplings of *P. nigra* and *Q. ilex* and on mature individuals of the annual herbaceous *H. annuus* ($n = 135$ per species). *P. nigra* and *Q. ilex* saplings were kindly provided by Dipartimento Regionale Azienda Foreste Demaniali (Messina, Italy). In February 2020, saplings were transferred to the campus of University of Messina, and planted in

3.4 L pots filled with forest topsoil collected from Colli San Rizzo (Messina, Italy). Seeds of *H. annuus* were planted in greenhouse trays at the end of April 2020 (n = 60) and at the beginning of May (n = 75) to assure availability of individuals of similar age over the whole experimental period (10–15 weeks old, before flowering). After the emergence of at least two developing leaves, seedlings were transferred in pots similar to those used for *Q. ilex* and *P. nigra*. All plants were grown in open-field conditions and regularly irrigated at field capacity every 2 days until early June, when they were transferred in a greenhouse to start the dehydration treatments. The greenhouse received only natural light, with maximum daily values of photosynthetic photon flux density averaging 1370 ± 300 µmol s^{-1} m^{-2} (h: 11:00–12:30). Day/night temperatures were 30°C/24°C and air relative humidity averaged 60%.

Plant dehydration was induced by two different procedures, i.e., bench-dehydration of uprooted plants, and dehydration in pots by suspending irrigation (Figure S1A). In the bench dehydration treatment, well-watered potted plants were initially enclosed in a plastic bag for at least 8 h (Figure S1B). This experimental procedure allowed us to obtain fully hydrated samples (Time 0). Samples were then gently pulled out of the pot. The soil was gently rinsed under water to avoid damages to the root system (Figure S1B). Then, the excess of water was quickly absorbed by paper towel and each sample was slowly allowed to dehydrate inside a large plastic bag humidified with damp paper towel, to prevent non-uniform transpiration (Figure S1A). In pot dehydration treatment, desiccation was obtained by withholding irrigation. In this case, at least two well-watered plants per each species were measured at pre-dawn, after maintaining pot samples inside a plastic bag during the whole night. In pot-dehydrated plants, root samples were obtained by easily removing dry soil from the root system, without using water. During the dehydration treatments, samples were maintained in the greenhouse.

2.2 | Estimating turgor loss point, gas exchange rates and leaf water potential

To quantify the species-specific leaf water potential at the turgor loss point (Ψ_{tlp}), water potential isotherms (i.e., pressure-volume curves) were measured on five leaves from different plants per species. Specifically, Ψ_{tlp} was estimated as the flex point of the relationship between the inverse value of leaf water potential ($1/\Psi_L$) as measured by a pressure chamber (PMS Instruments), and the cumulative water loss (Tyree & Hammel, 1972).

A portable LCi Analyzer System (ADC Bioscientific Ltd.) was used to measure leaf conductance to water vapour (g_L) in pot-dehydrated plants, just before collecting samples for water content measurements. Moreover, measurements of leaf water potential were also performed using the pressure chamber. Monitoring of gas exchange and leaf water potential values was performed until g_L values of about 10 mmol m^{-2} s^{-1} were recorded.

2.3 | Measurements of RWC and rehydration capacity

Measurements of RWC and percentage loss of rehydration capacity (PLRC) were performed on leaf, stem and root samples collected from pot-dehydrated and bench-dehydrated plants. At different dehydration times, leaf, 2-cm-long stem segments and primary root samples were cut by razor blade and immediately weighted to obtain their fresh weight (FW). Samples were then rehydrated by immersing them in distilled water for 8–12 h, and then their turgid weight (TW) was recorded. Stem and root samples were fully immersed in distilled water, while leaves were rehydrated by immersing only their petiole. Finally, samples were oven dried for 3 days at 70°C to obtain their dry weight (DW). Rehydration time was chosen on the basis of preliminary measurements showing that 8 h guaranteed full rehydration while avoiding oversaturation effects in all three species and organs. In detail, the weight of rehydrating leaf, stem and root samples at different dehydration levels (including well-watered samples, see below) was recorded hourly for 8 h, and then after 12 h and 24 h. In all three dehydrated species and organs, the maximum rehydration occurred within 8 h. Effects of oversaturation occurred, in some but not in all checked samples, after 12 h of rehydration (Figure S2). It can be noted that similar rehydration times were found suitable also for other species (Abate et al., 2021; John et al., 2018). The weight of well-watered samples used for estimating the saturated water content (see below) remained constant or increased by less than 3% compared to their initial weight within 8 h (on the basis of the organ and the species). Thus, for these samples we decided to consider as TW the weight recorded after maintaining them submerged for 1 h.

Commonly, RWC is estimated as: (FW-DW)/(TW-DW). However, in most severe dehydrated samples, RWC can be overestimated as a likely effect of the cell rehydration ability loss (Abate et al., 2021), leading to only small water content increment during rehydration. To check for this artefact in the three study species, we compared values of RWC as obtained by the most commonly used approach (see above) with values obtained on the basis of the use of saturated water content, as estimated on well watered samples (SWC_w), instead of TW. In detail, eight potted control plants per species (different from those used for pot-dehydration measurements) were fully irrigated the evening before the measurement and maintained enclosed in a plastic bag overnight (i.e., for at least 8 h). In the early morning, the FW of leaf, stem and root samples was recorded. Then, samples were immersed in distilled water for 1 h to obtain their TW (see above).

The SWC_w value of leaf, stem and root was estimated as:

$$SWC_w = (TW - DW)/DW.$$

The RWC values were then calculated on the basis of the saturated water content (RWC_{SWC}) as:

$$RWC_{SWC} = 100 \times WC_i/SWC_w$$

where WC_i is the water content of the dehydrated samples, i.e.:

$$WC_i = (FW - DW)/DW.$$

It should be noted that equations for the calculation of RWC based on TW following rehydration of water-stressed leaves, or on SWC_w, albeit apparently very different, are mathematically identical, with the difference that RWC_{SWC} calculation is based on 'average' values of (TW − DW) gathered on leaves that had never experienced water stress.

As reported in Figure S3, we found discrepancies between RWC values recorded by the traditional formula and those calculated using SWC, especially in most severely dehydrated samples. In these cases, estimating RWC by the traditional formula led to an overestimation of the value. Thus, we used RWC_{SWC} values that, from here on, are simply referred as RWC.

PLRC values were estimated as:

$$PLRC = 100 \times (1 - SWC_r/SWC_w)$$

where SWC_r is the saturated water content of dehydrated leaf, stem and root samples, as recorded after rehydration. In some watered samples, WC_i was higher than the SWC_w because it fell at the lower end of the range of the mean value. Based on this assumption, we considered the PLRC of these samples as 0.

Whole plant RWC was estimated by the proportion of each species-specific organ dry mass fraction, multiplied by their respective RWC (Sapes & Sala, 2021). After sampling leaf, stem and root for estimating water content and the REL (see below), remaining root, stem and leaf samples were oven dried for 3 days at 70°C to obtain their DW. Dry biomass of samples measured for water content was included into estimation of the whole plant RWC.

2.4 | Relative electrolyte leakage

To check for eventual detrimental effects of dehydration on the integrity of cell membranes, electrolyte leakage measurements were performed on leaf, stem and root samples collected at the same time and as near as possible to samples used for water content estimates. In detail, leaf samples of about 1 cm^2, 2-cm-long stem segments and primary root samples were cut with a razor blade and immediately placed in test tubes containing 8 ml of distilled water. Tubes were then stirred for 30 min and the initial electrical conductivity of the solution (EC_i) was recorded by a conductivity metre (Cond 5, XS instruments). Samples were then subjected to three freeze/thaw cycles (i.e., T = −20°C, +20°C) to induce membrane disruption and processed as above to estimate the final electrical conductivity of the solution (EC_f) (Petruzzellis et al., 2018; Savi et al., 2016). The REL was calculated as: $REL = (EC_i/EC_f) \times 100$.

2.5 | Plant mortality

A set of 55 plants per species was used to assess drought-driven plant death. Plants were divided in 5 groups of 11 individuals per species. In each group, at different days after the last irrigation (see below), three samples per species were measured for estimating the native RWC, PLRC and REL and the remaining eight samples were re-irrigated at field capacity to estimate their eventual recovery. The parameters were measured in well-watered samples, in samples experimenting turgor loss (as estimated by leaf water potential measurements), and in samples not irrigated for additional 2, 4 and 6 days (*H. annuus* samples) and 5, 10, 15 days (*P. nigra* and *Q. ilex* samples) after reaching (and surpassing) the turgor loss point. Samples were considered dead if, after 10 (sunflower plants) or 40 days (poplar and oak seedlings) after re-irrigation, their canopy was still completely dry and no new sprouts had appeared (Figure S1C). This experimental procedure was completed within the first week of August 2020.

2.6 | Statistical analysis

The main aims of our analysis were to test eventual differences: (i) in the relationships between RWC, PLRC and REL between a fast-experimental dehydration (i.e., bench dehydration) and a long-term water stress (i.e., pot dehydration) and (ii) in specific RWC thresholds among organs. In this light, we developed a two-steps framework. We first investigated possible differences in general trends between dehydration types, and then we tested whether they resulted in different specific RWC, PLRC and REL thresholds (see Tables S1–S3). The above-mentioned relationships were assessed by fitting both generalised least square (*gls*) and generalised nonlinear models (*gnls*) through *gls* and *gnls* function in "nlme" package (Pinheiro et al., 2016) for R software (R Core Team, 2022) and *drm* function in "drc" (Ritz et al., 2015) R package. Specifically, *gls* function was used to fit generalised least square models to test the relationship between PLRC and REL, while *gnls* function was used to fit two-parameter exponential models to test the relationships between RWC and REL, and *drm* function was used to fit a three-parameter log-logistic model to test the relationships between PLRC and RWC. For each relationship tested, we choose the model type showing the best fitting (i.e., higher R^2) after a preliminary analysis.

For PLRC and REL relationship, a *gls* was fitted independently for each species by setting PLRC as the response variable and REL, dehydration type, organ and their interactions as the explanatory ones. To meet homogeneity of variances assumption, a varPower variance structure was specified in each tested model. When significant interactions between REL, dehydration type and organ were found, estimated marginal means of linear trends were calculated using *emtrends* function in "emmeans" (Lenth, 2022) R package. For non-linear relationships (i.e., PLRC vs. RWC, and REL vs. RWC), we followed the procedure described in Ritz and Streibig (2009). Two non-linear models were fitted for each species and

organ: in the first one, data were pooled together, while in the second one dehydration type was included as a grouping factor. The two models were then compared by means of a *F* test (for two-parameter exponential models) and a likelihood-ratio test (for three-parameter log-logistic models) using *ANOVA* function in "car" R package, and differences between dehydration types were considered significant when the *F* test resulted in a *p* value lower than 0.05 and when the model considering dehydration type as a grouping factor had the lowest residual sum of squares or Akaike Informative Criterion value. This step allowed to assess possible differences in general trends of the tested relationship but did not allow to assess whether different trends resulted in different physiological thresholds. In this light, we developed a bootstrap procedure to calculate specific RWC, PLRC and REL thresholds (see Tables S1–S3) for each relationship tested using a custom-made R function. Specifically, for each species and for each organ we resampled data points at random with replacement, we fitted the same model type calculated in the first step of the framework and we calculated the specific thresholds reported in Tables S12–S16 using *approx* function in "stats" R package. This procedure was repeated 999 times after which the mean values of each physiological threshold and associated 95% confidence intervals (CI) were calculated. Differences between dehydration types, species and organs were considered statistically significant when the 95% CI did not overlap.

A similar framework was applied also to test the third and the fourth aims of our study, which were to investigate the coordination between whole plant, leaf, stem and root RWC, PLRC and REL with stomatal closure and plant mortality. In this light, three-parameter log-logistic model were used to assess the relationships between g_L versus Ψ and g_L versus RWC in each organ and in each species, as well as g_L versus RWC_{plant} in each species, through *drm* function. Exponential decay and logarithmic models were fitted to assess the relationships between g_L versus PLRC and g_L versus REL, respectively. At last, two parameters exponential models were fitted to assess the relationship between plant mortality and RWC, plant mortality and PLRC and plant mortality and REL in each organ and in each species using *gnls* function. Differences in Ψ, RWC, PLRC and REL values inducing 20%, 50% and 80% loss of g_L and in RWC, PLRC and REL values inducing 10% and 50% plant mortality among species were assessed using a similar framework as the one described above. In this case, species (and not dehydration type) was considered the grouping factor (Tables S4–S10, S17–S19).

3 | RESULTS

As expected, in all species bench-dehydration of uprooted plants occurred at a faster rate compared to dehydration of potted plants (Figure S4, Table S11). Overall, whole dehydration of *H. annuus* samples occurred within 11 days when pot-dehydrated, and within only 2–3 days (i.e., about 60 h) when bench-dehydrated. Similarly, *P. nigra* and *Q. ilex* samples lost their total water content in about 25 days when pot-dehydrated, but only within 4 days (i.e., about 100 h) when bench-dehydrated. It can be noted that root dehydration occurred very quickly (within 10 h) and faster than leaf and stem dehydration in uprooted plants. By contrast, root dehydration occurred at similar rate of leaf and stem dehydration in potted plants, in all the study species. Nevertheless, the two dehydration treatments produced similar results, as shown by overlapping trends of relationships between species-specific leaf, stem and root PLRC to RWC (Figure 1, Tables S1 and S12), PLRC to REL (Figure 2, Tables S2 and S13) and REL to RWC (Figure 3, Tables S3 and S16) in bench- versus pot-dehydrated samples.

Declining RWC induced a progressive loss of leaf, stem and root rehydration capacity (Figure 1). In detail, in *H. annuus* a statistically similar RWC value inducing 10% PLRC was recorded for all plant organs (i.e., RWC_{PLRC10} ~65%, Figure 1, Table 1, Table S12). Lower RWC values inducing 25% PLRC were recorded in leaf compared to stem and root for sunflower samples (i.e., RWC_{PLRC25} ~35% vs. 48%, respectively). In *P. nigra*, similar RWC_{PLRC10} values were recorded for leaves and roots (i.e., about 80%), while stems showed a RWC_{PLRC10} of about 65%, (i.e., lower than the threshold measured in the leaves but statistically similar to that of roots, Figure 1, Table 1, Table S12). Moreover, statistically higher RWC_{PLRC25} in leaves versus stems and roots (i.e., 58% vs. 37%, respectively) was recorded in this species. Leaf and stem samples of *Q. ilex* showed similar RWC_{PLRC10} values (i.e., about 65%); roots showed higher values than those recorded for stems, but statistically similar to leaves (i.e., ~70%, Figure 1, Table 1, Table S12). In this species, the RWC_{PLRC25} was about 39% for all three organs.

Drought-driven loss of rehydration capacity strongly depended on cell membrane damage, as indicated by robust correlations between PLRC and REL recorded in all three species and organs (Figure 2, Table S2). In fact, in all three species and organs, the relationship between PLRC and REL was linear and close to 1:1. Moreover, cell membrane damage correlated to water content according to an exponential behaviour (Figure 3, Table S3). Hence, the initial decline in water content did not produce any membrane damage, and REL increased only at RWC values below 75%. Linear correlations were recorded between the species-specific whole-plant RWC and leaf, stem and root PLRC and REL (Figure S5, Table S14, S15).

Robust correlations were also recorded between stomatal conductance to water vapour and water status (Figure 4, Table 1, Table S4). As expected, g_L decreased in response to dehydration. In accordance, significant correlations between g_L and leaf water potential as well as between g_L and leaf RWC were recorded in all the study species. *P. nigra*, where the higher vulnerability in terms of PLRC was recorded (Figure 1, Table S12), showed the fastest stomatal response to dehydration among the study species (Figure 4). In this species, substantial stomatal closure occurred at leaf water potential higher than the turgor loss point (i.e., −1.1 MPa vs. −2.1 MPa), while in *H. annuus* and *Q. ilex* the water potential leading to 80% loss of g_L (P_{gL80}) was similar to the species-specific turgor loss point. Moreover, all organs of *H. annuus*, stem and root of *P. nigra*, as well as leaf and stem of *Q. ilex* showed similar RWC values leading to

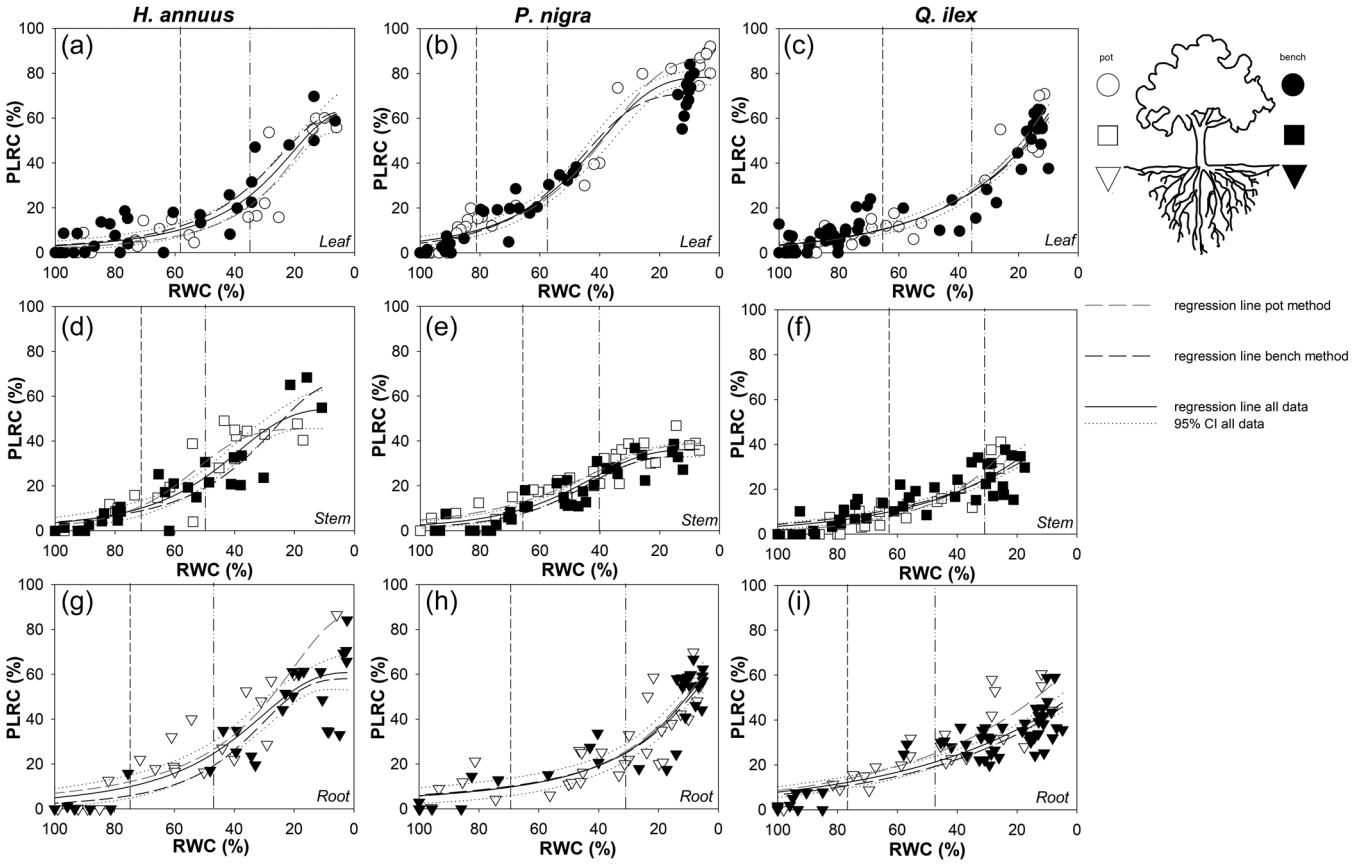

FIGURE 1 Relationships between the percentage loss of rehydration capacity (PLRC) and the relative water content (RWC) of dehydrating leaf (circles), stem (squares) and root (triangles) samples as recorded by pot (white symbols) and bench (dark symbols) dehydration treatments in (a, d, g) *H. annuus*, (b, e, h) *P. nigra* and (c, f, i) *Q. ilex*. Long dash lines show the best fitted regression curve of pot (dark lines) and bench (grey) leaf, stem and root samples. Black solid and dotted lines show, respectively, the regression curve and associate 95% CIs as obtained by fitting all data recorded by pot and bench dehydration treatments. Vertical lines indicate RWC value leading to 10% PLRC (RWC_{PLRC10}, short dash line) and RWC value leading to 25% PLRC (RWC_{PLRC25}, dash dot dot line). For details on method and fitted curves, see the text and Table S1. CI, confidence interval.

80% loss of g_L (i.e., RWC_{gL80} ~70%, Figure 4, Table 1, Table S17). By contrast, in *P. nigra* leaf RWC_{80gL} was as high as about 87%, 95% CIs (84, 89) (Figure 4 and Table 1). Similar plant-level RWC values leading to severe stomatal closure were recorded in the three species. In accordance, plant RWC values of about 70%, led to 80% loss of g_L (Figure 4 and Table S17).

According to CIs overlap, drought-driven stomatal closure was also coupled to changes in PLRC. Leaf PLRC ~10% as well as root PLRC of about 18% was associated to g_L loss of about 80% in all three study species (Figure 5, Table 1, Table S18). Moreover, leaf membrane damage, especially at leaf and root level, followed stomatal closure in all the study species. In fact, REL values of about 20% (for all sunflower organs and leaf poplar samples) and about 35% (for stem and root *P. nigra* and all *Q. ilex* organs) occurred after an 80% reduction of stomatal conductance had been recorded (Figure 5, Table 1, Table S18).

Plant mortality was clearly correlated to water status (Figure 6, Table 1, Table S19). RWC decline was a reliable proxy of plant mortality risk in all the study species, regardless of the specific organ considered. In fact, similar leaf, stem and root as well as whole-plant RWC values of about 60% led to 10% plant mortality in the two woody species (i.e., *P. nigra* and *Q. ilex*) as well as in sunflower where, however, slightly higher RWC thresholds were detected at whole plant level (Figure 6, Table S19). We also assessed the RWC threshold leading to 50% of plant mortality (RWC_{M50}). In sunflower, 50% of plant mortality was recorded at whole plant RWC values of about 35%, while in *P. nigra* and *Q. ilex* plants, RWC_{50M} was about 15% (Table S19). Moreover, differences among organs in RWC_{M50} values were recorded.

Correlations were recorded between plant mortality and leaf, stem and root PLRC as well as between plant mortality and REL values (Figure S6, Table S19). In particular, a PLRC of about 10% and a REL of about 18% led to 10% plant mortality in sunflower samples. Higher values were recorded in the two woody species where similar leaf PLRC of about 18% and REL of about 25% triggered plant mortality. Moreover, similar stem and root PLRC values of approximately 10% and 18%, respectively, led to 10%

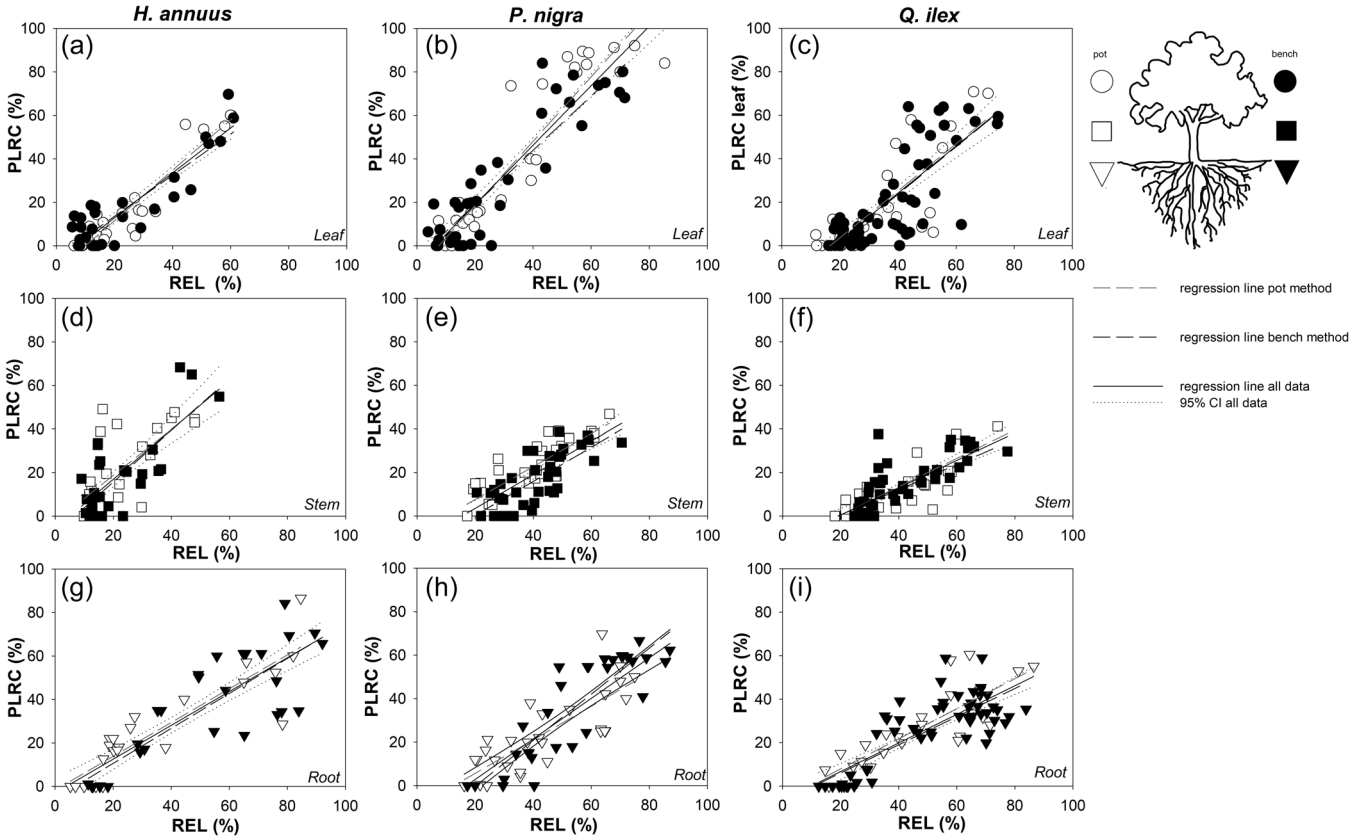

FIGURE 2 Relationships between the percentage loss of rehydration capacity (PLRC) and the relative electrolyte leakage (REL) of dehydrating leaf (circles), stem (squares) and root (triangles) samples as recorded by pot (white symbols) and bench (dark symbols) dehydration treatments in (a, d, g) *H. annuus*, (b, e, h) *P. nigra* and (c, f, i) *Q. ilex*. Long dash lines show the best fitted regression curve of pot (dark lines) and bench (grey) leaf, stem and root samples. Black solid and dotted lines show, respectively, the regression curve and associated 95% CIs as obtained by fitting all data recorded by pot and bench dehydration treatments. For details on method and fitted curves, see the text and Table S2. CI, confidence interval.

plant mortality in all study species. Overall, our data suggest that RWC values are better predictors of the risk of mortality compared to PLRC and REL, whose robustness of predictive power depended on species-specific organs (Tables S6, S9 and S10).

4 | DISCUSSION

Our results strongly support the hypothesis that RWC can be used as a reliable proxy to evaluate the risk of drought-driven plant mortality. In fact, leaf, stem and root RWC decline in response to water shortage were robust indicators of increased risk of plant die-off in all the study species. In accordance, similar RWC values of about 60% led to 10% plant mortality in the study species. Moreover, water content related parameters as PLRC and REL proved to be good indicators of plant mortality risk as well. Interestingly, similar PLRC and REL thresholds for drought-driven plant death were recorded in woody species. Similar stem and root PLRC values of 10% and 18%, respectively, led to 10% plant mortality in all study species.

4.1 | Estimating RWC

In this study, we initially tested the reliability of RWC values calculated using a traditional approach to estimate TW, compared to the use of saturated water content values recorded in well hydrated plants/organs. In fact, at species-specific water content threshold, cells lose their rehydration ability (i.e., Abate et al., 2021; John et al., 2018; Trueba et al., 2019), leading to possible underestimation of TW and overestimation of RWC. Results recorded in leaf, stem and root samples of our study species confirmed this risk, with consistent overestimation of RWC calculated using classical approaches. We recorded a 1:1 correlation between the two differently estimated values of RWC only until initial loss in cell rehydration capacity occurred, with values diverging after this critical point (Figure S3). The risk of undersaturation following rehydration was higher in *H. annuus* (all organs) as well as in *P. nigra* and *Q. ilex* leaves and roots. A similar result was recorded in a previous study on two *Salvia* species (Abate et al., 2021), and confirms the need to consider dehydration-driven damages to cells in studies aimed to quantify variations in RWC under drought. Of course, estimates of RWC based on SWC are not fully free of artefacts, especially when it is not

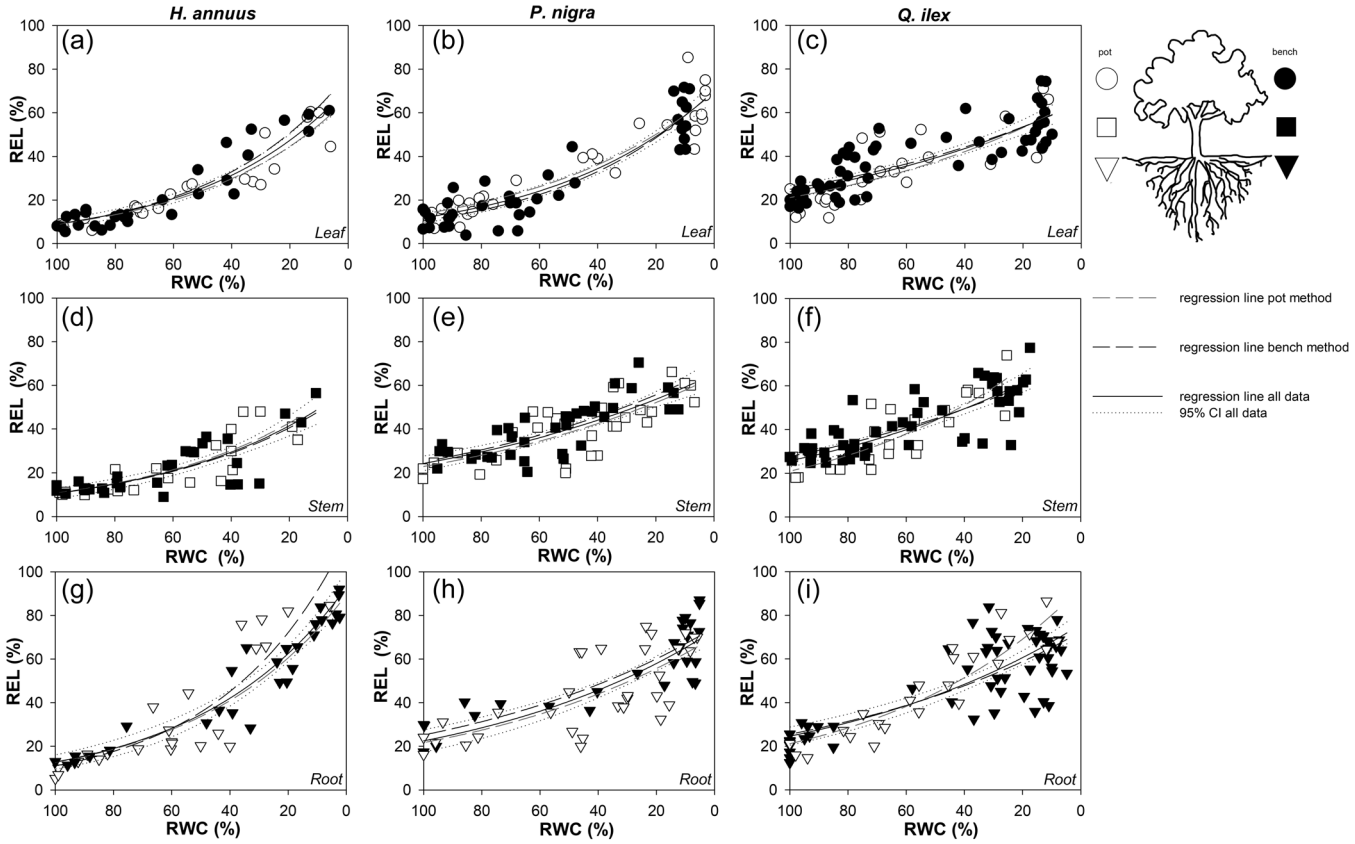

FIGURE 3 Relationships between the relative electrolyte leakage (REL) and the relative water content (RWC) of dehydrating leaf (circles), stem (squares) and root (triangles) samples as recorded by pot (white symbols) and bench (black symbols) dehydration treatments in (a, d, g) *H. annuus*, (b, e, h) *P. nigra* and (c, f, i) *Q. ilex*. Long dash lines show the best fitted regression curve of pot (dark lines) and bench (grey) leaf, stem and root samples. Black solid and dotted lines show, respectively, the regression curve and associated 95% CIs as obtained by fitting all data recorded by pot and bench dehydration treatments. For details on method and fitted curves, see the text and Table S3. CI, confidence interval.

possible estimate the SWC_w on the same sample where dehydration is imposed, and/or in not homogenous plant material. Nevertheless, in the present study, as likely consequence of similar provenance, age, soil type, and growth condition, the variability in SWC values was low (no more than ± 10% of the mean value).

We tested different experimental procedures for sample dehydration. Bench dehydration of uprooted plants or detached branches is commonly used to induce xylem embolism and quantify drought-driven hydraulic conductance decline (i.e., Cochard et al., 2013; John et al., 2018; Kiorapostolou et al., 2019). This experimental procedure has the relevant advantage to allow obtaining samples at low water content quickly, thus shortening the time required for measurements. Nevertheless, such a fast dehydration may cause artefactual results when quantifying critical water content thresholds leading to irreversible plant failure. In fact, fast dehydration may hamper possible biochemical and physiological time-dependent acclimation processes, and/or whole plant coordinated responses that are likely to occur in plants experiencing more 'natural' long-term decline of their water content. However, our data revealed a very good agreement between results recorded by bench versus pot dehydration. Independently on the method used, similar declines in PLRC as a function of RWC were recorded, and we also observed similar relationships of RWC with REL. Therefore, we conclude that fast bench dehydration is a reliable procedure to assess species-specific water content thresholds leading to membrane damage and loss of rehydration capacity, that in turn predispose plants to irreversible failure.

4.2 | Leaf, stem and root RWC thresholds for membrane damage and stomatal closure

In all the study species, RWC and PLRC, as well as membrane damage in terms of REL, were strongly correlated to stomatal closure. A statistically similar plant RWC of about 70%, leaf and root PLRC values of about 10% and 18%, respectively, as well as a root REL of about 34% was associated to 80% stomatal closure in all the species. Correlations between leaf water status and gas exchange are widely reported in literature since the leaf water content directly affects stomatal aperture (i.e., Brodribb & McAdam, 2017; Sperry, 2000; Trifilò et al., 2003). By contrast, links between stem and/or root water status and stomatal behaviour have been mainly obtained indirectly, by hydraulic conductance estimation (i.e., Bartlett et al., 2016). Our findings

TABLE 1 Values of leaf, stem and root relative water content (RWC), leaf water potential (P), percentage loss of rehydration capacity (PLRC) and relative electrolyte leakage (REL) as measured in dehydrating plants of *H. annuus*, *P. nigra* and *Q. ilex*.

	Helianthus annuus			*Populus nigra*			*Quercus ilex*		
	Leaf	**Stem**	**Root**	**Leaf**	**Stem**	**Root**	**Leaf**	**Stem**	**Root**
RWC_{PLRC10} (%)	58.9 (51–67)	71.4 (65–77)	75.1 (65–87)	82.1 (77–93)	64.8 (61–69)	69.5 (56–84)	64.7 (58–74)	62.5 (58–67)	76.5 (71–83)
RWC_{PLRC25} (%)	35.4 (30–41)	48.8 (44–55)	46.5 (41–53)	58.1 (52–61)	40.1 (37–43)	31.2 (26–37)	36.4 (31–42)	33.6 (26–39)	47.4 (39–57)
$-P_{gL80}$ (MPa)	1.1 (0.8–1.2)	–	–	1.1 (1.0–1.2)	–	–	2.5 (1.5–3.5)	–	–
RWC_{gL80} (%)	67.9 (64–72)	71.5 (56–81)	64.5 (59–70)	86.8 (84–89)	69.7 (64–73)	71.6 (56–82)	72.8 (69–78)	68.9 (65–73)	55.9 (51–63)
$PLRC_{gL80}$ (%)	7.8 (3–14)	19.7 (8–36)	21.2 (14–32)	9.7 (8–12)	15.3 (10–20)	9.3 (4–18)	7.3 (4–10)	6.6 (1–13)	21 (15–28)
REL_{gL80} (%)	19.9 (18–22)	18.5 (15–21)	26.9 (20–31)	17.0 (12–20)	36.5 (26–45)	34.0 (28–41)	34.8 (21–47)	36.4 (29–45)	41.7 (34–52)
RWC_{10M} (%)	61.1 (55–67)	66.6 (46–86)	68.8 (57–84)	49.9 (39–65)	54.5 (41–75)	45.2 (31.9–69)	56.5 (50–67)	59.2 (47–73)	44.6 (34–60)
RWC_{50M} (%)	26.5 (25–31)	40.9 (36–48)	37.2 (33–41)	11.9 (9–18)	20.1 (17–24)	16.1 (14–19)	17.5 (14–21)	30.9 (38–37)	16.4 (13–20)
$PLRC_{10M}$ (%)	7.1 (4–10)	11.2 (6–18)	14.4 (10–20)	22.6 (17–29)	14.7 (10–21)	12.8 (6–19)	15.2 (11–20)	6.5 (1–11)	23.2 (16–30)
REL_{10M} (%)	17.9 (15–21)	16.3 (14–19)	18.4 (12–25)	24.8 (19–30)	28.9 (25–34)	31.5 (26–38)	28.9 (24–34)	34.0 (27–40)	39.7 (33–50)

Note: Confidence intervals are shown in brackets. RWC_{PLRC10} and RWC_{PLRC25}: RWC values leading to 10 and 25 PLRC; P_{gL80}: water potential values leading to 80% loss of stomatal conductance to water vapour (g_L); RWC_{gL80}: RWC values leading to 80% loss of stomatal conductance to water vapour (g_L); $PLRC_{gL80}$: PLRC values leading to 80% loss of stomatal conductance to water vapour (g_L); REL_{gL80}: REL values leading to 80% loss of stomatal conductance to water vapour (g_L); RWC_{10M} and RWC_{50M}: RWC values leading to 10% and 50% of plant mortality; $PLRC_{10M}$: PLRC values leading to 10% of plant mortality; REL_{10M}: REL values leading to 10% of plant mortality.

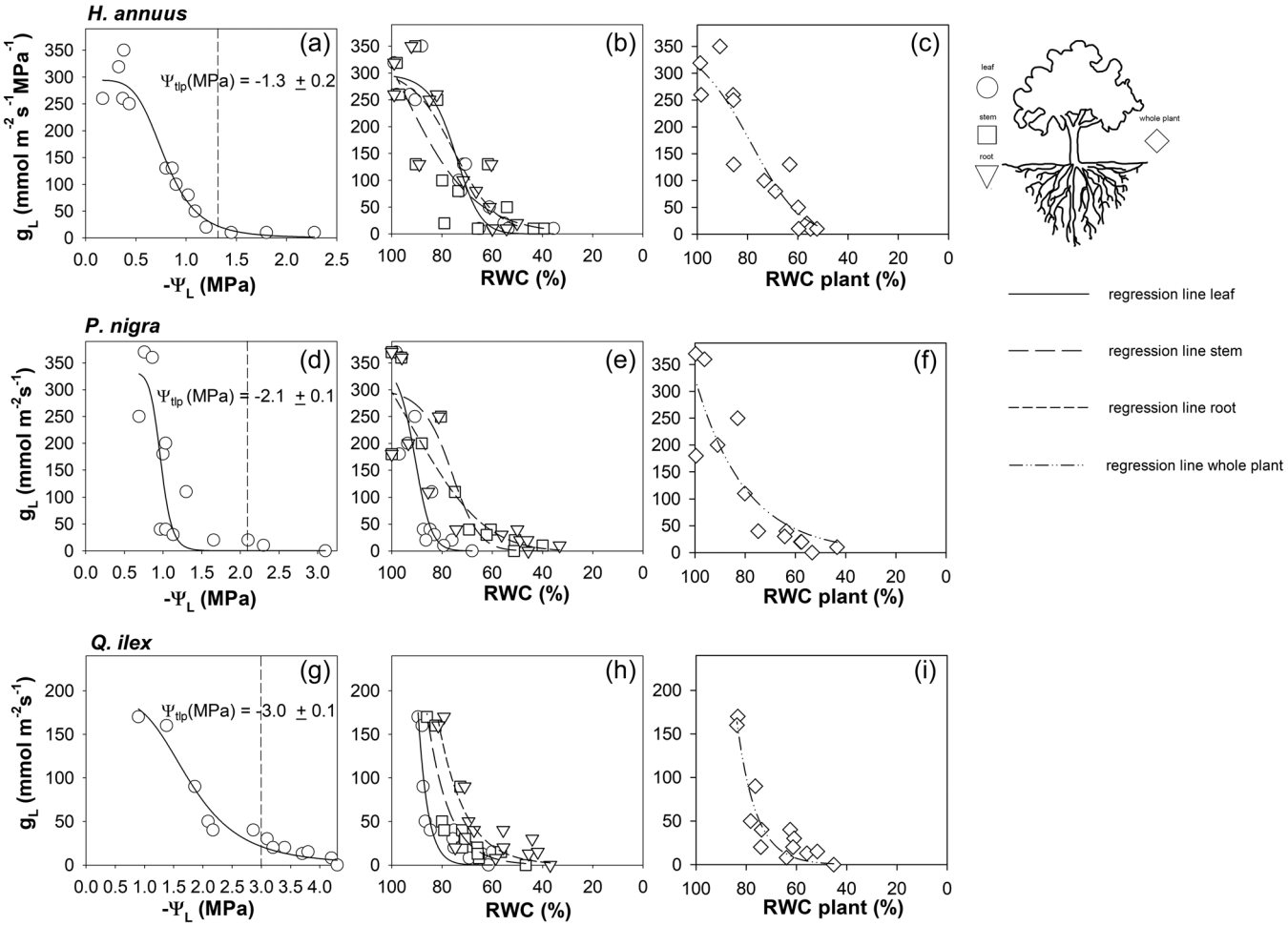

FIGURE 4 Relationships between stomatal conductance to water vapour (g_L) and leaf water potential (Ψ_L) and between g_L and relative water content (RWC) of dehydrating leaf (circles), stem (squares), root (triangles) and whole plant (diamond) samples as recorded by pot dehydration treatment in (a–c) *H. annuus*, (d–f) *P. nigra* and (g–i) *Q. ilex*. Solid, long dash, short dash and dash-dot-dot lines show the regression curve as obtained for leaf, stem, root and whole plants, respectively (for details on fitted curves, see Table S4). Mean values ± *SD* of the species-specific leaf water potential at turgor loss point (Ψ_{tlp}) are reported and indicated by the vertical short dash lines.

strongly suggest coordination among water content of all plant organs and stomatal behaviour. However, more robust correlations were recorded when considering water content at leaf and root level. Previous studies have suggested a key role of root systems in stomatal regulation via chemical signalling, hydraulic conductance changes and drought-driven damage (i.e., Cuneo et al., 2016; Rodriguez-Dominguez & Brodribb, 2020; Tardieu et al., 2017). Indeed, the root is a primary drought-sensing organ, and increased accumulation of reactive oxygen species in roots under drought has been documented (i.e., Alam et al., 2010; Mukarram et al., 2021; Zhao et al., 2001). Hence, it is reasonable to hypothesise that drought-driven changes in root RWC and, as a consequence, in membrane damages, while leading to loss of rehydration capacity, might also trigger (chemical) signals involved in gas exchange regulation.

In all the study species, the leaf RWC_{PLRC10} corresponded to the RWC threshold leading to 80% drop of stomatal conductance. In fact, statistically similar RWC of about 65%–70% in *H. annuus* and *Q. ilex* leaf, and of about 85% in *P. nigra* leaf, were related to 10% PLRC as well as to 80% loss of g_L. Moreover, in all three study species the increase in cell membrane damage corresponding to REL values of 20%–30% was observed at 80% loss of stomatal conductance. In other words, decline in gas exchange occurred in response to water status but before the initial loss of cells' rehydration capacity. These results suggest that, despite stomatal closure to limit further water loss, dehydration continued leading to membrane damages which, in turn, resulted in the loss of rehydration ability. Our data are in agreement with Trueba et al. (2019), reporting a similar sudden stomatal closure after the initial loss of leaf rehydration capacity, which, in turn, occurred before any decline in photochemical efficiency.

If confirmed in other species, these values of PLRC of about 10% and REL of 20%–30% might represent reliable indicators of the critical water content threshold leading to membrane damage and decline of carbon assimilation.

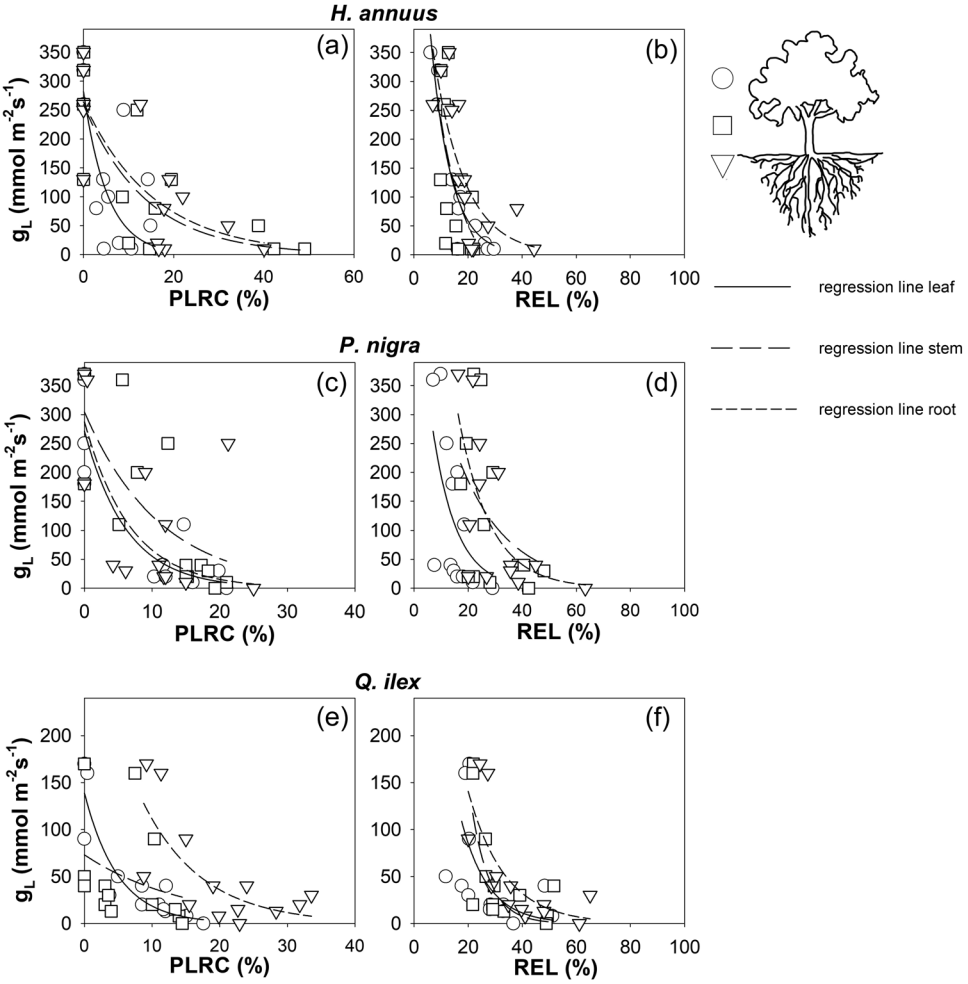

FIGURE 5 Relationships between stomatal conductance to water vapour (g_L) and the percentage loss of rehydration capacity (PLRC) and between g_L and relative electrolyte leakage (REL) of dehydrating leaf (circles), stem (squares) and root (triangles) samples as recorded by pot dehydration treatment in (a, b) *H. annuus*, (c, d) *P. nigra* and (e, f) *Q. ilex*. Solid, long dash and short dash lines show the regression curve as obtained for leaf, stem and root, respectively. For details on fitted curves see Table S5

4.3 | RWC, PLRC and REL as reliable parameters for predicting plant die-off risk

The possible use of RWC as an indicator of plant mortality risk has received increasing attention in the last years (Martinez-Vilalta et al., 2019). In accordance, plant water content reliably predicted the mortality risk of *Pinus ponderosa* seedlings (Sapes & Sala, 2021), and integrated information on drought-driven hydraulic failure and carbon starvation in this species (Sapes et al., 2019). Here, we report robust correlations between RWC and plant mortality in three different species with very different growth forms and leaf habits, supporting the use of RWC as an easy-to-measure trait predicting the risk of plant decline compared to other measurements. Such correlations between RWC and mortality were overall good, regardless of the organ considered. Moreover, the initial increase in plant mortality rates (i.e., >10% plant mortality) occurred at the same RWC value in both herbaceous and woody species (i.e., RWC ~60%). Not last, mortality was also associated to 10%–15% loss of rehydration ability of leaf, stem and root cells, suggesting that cell damage and loss of rehydration capacity are key events in the process leading to plant death (Mantova et al., 2021). These findings are in agreement with recent studies. Sapes and Sala (2021) reported that, in seedlings of *Pinus ponderosa*, a probability of 10% mortality occurred at the similar plant RWC value recorded in the present study, i.e., about 65%. John et al. (2018) reported that RWC leading to 10% of leaf PLRC changed as a function of leaf habitus, but also at increasing levels of aridity experienced during the growing season by 89 different species. In summary, values of plant RWC lower than about 60%, as well as values of PLRC >10% come to light as alarming thresholds for an abrupt increased risk of plant mortality.

5 | CONCLUSIONS

Our data provide evidence for RWC thresholds leading to increased risk of plant mortality. Despite the expected variation at organ level, there was substantial convergence toward a critical RWC = 60%

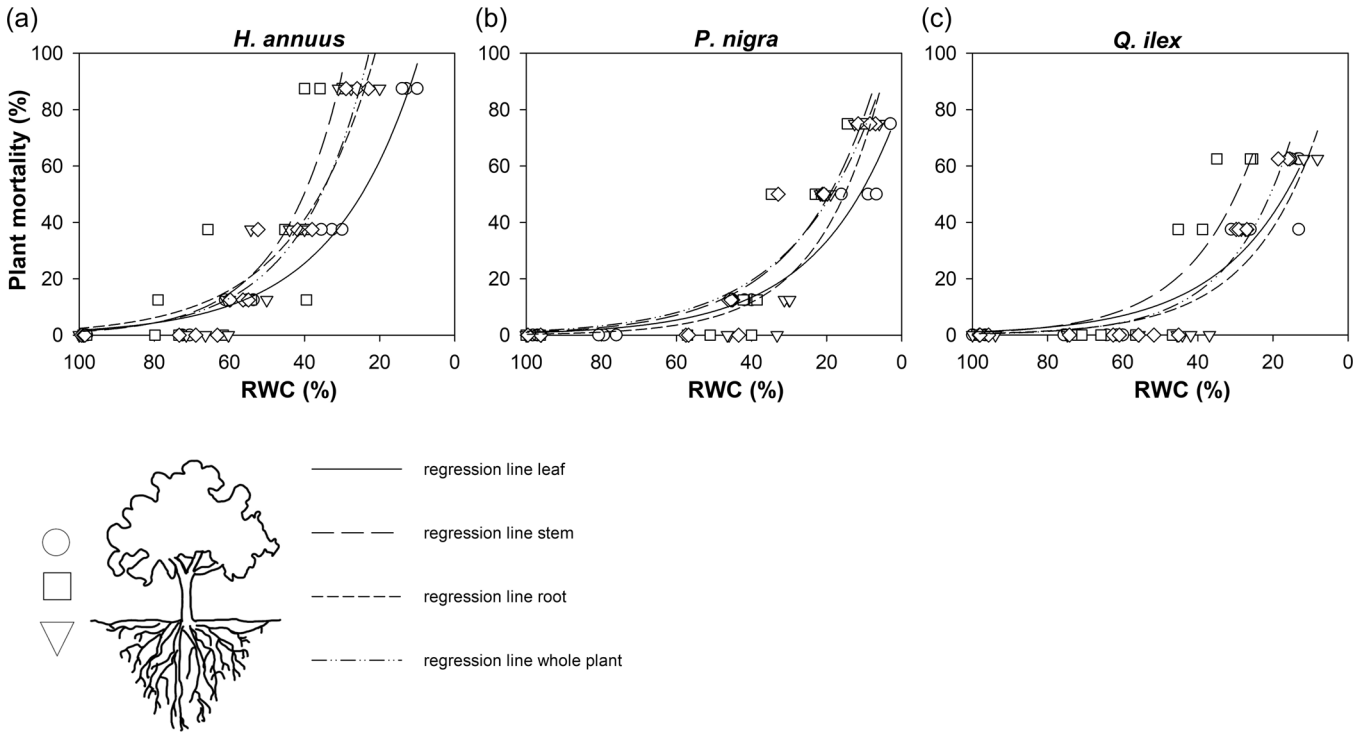

FIGURE 6 Relationships between percentage of plant mortality and relative water content (RWC), as recorded in leaf (circles), stem (squares) and root (triangles) and whole plants (diamond) of (a) *H. annuus*, (b) *P. nigra* and (c) *Q. ilex*. Solid, long dash, short dash and dash-dot-dot lines show the regression curve as obtained for leaf, stem, root and whole plants, respectively (for details on fitted curves, see Table S6).

leading to initial loss of rehydration capacity (PLRC ranging between 10% and 20%), possibly related to membrane damage as revealed by increasing REL values. Most interestingly, this critical RWC threshold apparently encompassed growth forms and leaf habits of the three study species, making this approach very promising for large scale and remote assessment of critical water status of vegetation, regardless of specific composition. It must be noted that our results were obtained on potted plants and, in the case of the woody species, on young saplings. Hence, the validity of the findings for field-growing and/or adult plants should be further investigated in future studies.

ACKNOWLEDGEMENTS

This research was supported by Finanziamento Attività di Base della Ricerca di Ateneo (FFABR Unime) 2020. We are very grateful to Dipartimento Regionale Azienda Foreste Demaniali, Messina, Sicily, Italy, for kindly providing plant material. We warmly thank Dr. Gerard Sapes and an anonymous reviewer for their careful reading of manuscript and insightful comments and suggestions.

CONFLICT OF INTEREST

The authors declare no conflicts of interest.

DATA AVAILABILITY STATEMENT

The data that support the findings of this study are available from the corresponding author upon reasonable request.

REFERENCES

Abate, E., Nardini, A. & Trifilò, P. (2021) Too dry to survive: leaf hydraulic failure in two *Salvia* species can be predicted on the basis of water content. *Plant Physiology and Biochemistry*, 166, 215–224.

Abdalla, M., Ahmed, M.A., Cai, G., Wankmüller, F., Schwartz, N., Litig, O. et al. (2021) Stomatal closure during water deficit is controlled by below-ground hydraulics. *Annals of Botany*, 129, 161–170.

Alam, I., Lee, D., Kim, K., Park, C., Sharmin, S.A., Lee, H. et al. (2010) Proteome analysis of soybean roots under waterlogging stress at an early vegetative stage. *Journal of Bioscience*, 35, 49–62.

Allen, C.D., Breshears, D.D. & Mcdowell, N.G. (2015) On underestimation of global vulnerability to tree mortality and forest die-off from hotter drought in the anthropocene. *Ecosphere*, 6, 129.

Allen, C.D., Macalady, A.K., Chenchouni, H., Bachelet, D., McDowell, N., Vennetier, M. et al. (2010) A global overview of drought and heat-induced tree mortality reveals emerging climate change risks for forests. *Forest Ecology and Management*, 259, 660–684.

Arend, M., Link, R.M., Patthey, R., Hoch, G., Schuldt, B. & Kahmen, A. (2021) Rapid hydraulic collapse as cause of drought-induced mortality in conifers. *Proceedings of National Academy of Sciences of the United States of America*, 118, e2025251118.

Barigah, T.S., Charrier, O., Douris, M., Bonhomme, M., Herbette, S., Améglio, T. et al. (2013) Water stress-induced xylem hydraulic failure is a causal factor of tree mortality in beech and poplar. *Annals of Botany*, 112, 1431–1437.

Bartlett, M.K., Klein, T., Jansen, S., Choat, B. & Sack, L. (2016) The correlations and sequence of plant stomatal, hydraulic, and wilting responses to drought. *Proceedings of the National Academy of Sciences USA*, 113, 13098–13103.

Brodribb, T.J. & Holbrook, N.M. (2004) Stomatal protection against hydraulic failure: a comparison of coexisting ferns and angiosperms. *New Phytologist*, 162, 663–670.

Brodribb, T.J., Holbrook, N.M., Zwieniecki, M.A. & Palma, B. (2005) Leaf hydraulic capacity in ferns, conifers and angiosperms: impacts on photosynthetic maxima. *New Phytologist*, 165, 839–846.

Brodribb, T.J. & McAdam, S.A.M. (2017) Evolution of the stomatal regulation of plant water content. *Plant Physiology*, 174, 639–649.

Carminati, A. & Javaux, M. (2020) Soil rather than xylem vulnerability controls stomatal response to drought. *Trends in Plant Science*, 25, 868–880.

Choat, B., Brodribb, T.J., Brodersen, C.R., Duursma, R.A., Lopez, R. & Medlyn, B.E. (2018) Triggers of tree mortality under drought. *Nature*, 558, 531–539.

Cochard, H., Badel, E., Herbette, S., Delzon, S., Choat, B. & Jansen, S. (2013) Methods for measuring plant vulnerability to cavitation: a critical review. *Journal of Experimental Botany*, 64, 4779–4791.

Cuneo, I.F., Knipfer, T., Brodersen, C.R. & McElrone, A.J. (2016) Mechanical failure of fine root cortical cells initiates plant hydraulic decline during drought. *Plant Physiology*, 172, 1669–1678.

Davis, S.D., Ewers, F.W., Sperry, J.S., Portwood, K.A., Crocker, M.C. & Adams, G.C. (2002) Shoot dieback during prolonged drought in *Ceanothus* (Rhamnaceae) chaparral of California: a possible case of hydraulic failure. *American Journal of Botany*, 89, 820–828.

Goulart, H., van der Wiel, K., Folberth, C., Balkovič, J. & van den Hurk, B. (2021) Storylines of weather-induced crop failure events under climate change. *Earth System Dynamics*, 12, 1503–1527.

Guadagno, C.R., Ewers, B.E., Speckman, H.N., Aston, T.L., Huhn, B.J., DeVore, S.B. et al. (2017) Dead or alive? Using membrane failure and chlorophyll a fluorescence to predict plant mortality from drought. *Plant Physiology*, 175, 223–234.

Hammond, W.M., Yu, K., Wilson, L.A., Will, R.E., Anderegg, W.R.L. & Adams, H.D. (2019) Dead or dying? Quantifying the point of no return from hydraulic failure in drought-induced tree mortality. *New Phytologist*, 223, 1834–1843.

Hartmann, H., Moura, C.F., Anderegg, W.R.L., Ruehr, N.K., Salmon, Y., Allen, C.D. et al. (2018) Research frontiers for improving our understanding of drought-induced tree and forest mortality. *New Phytologist*, 218, 15–28.

Hartmann, H., Ziegler, W., Kolle, O. & Trumbore, S. (2013) Thirst beats hunger—declining hydration during drought prevents carbon starvation in Norway spruce saplings. *New Phytologist*, 200, 340–349.

Hochberg, U., Windt, C.W., Ponomarenko, A., Zhang, Y.J., Gersony, J., Rockwell, F.E. et al. (2017) Stomatal closure, basal leaf embolism and shedding protect the hydraulic integrity of grape stems. *Plant Physiology*, 174, 764–775.

IPCC. (2013) Summary for policymakers, *Climate change 2013: the physical science basis*. Cambridge, UK: Cambridge University Press.

John, G.P., Henry, C. & Sack, L. (2018) Leaf rehydration capacity: associations with other indices of drought tolerance and environment. *Plant Cell & Environment*, 41, 2638–2653.

Kiorapostolou, N., Da Sois, L., Petruzzellis, F., Savi, T., Trifilò, P., Nardini, A. et al. (2019) Vulnerability to xylem embolism correlates to wood parenchyma fraction in Angiosperms but not in Gymnosperms. *Tree Physiology*, 39, 1675–1684.

Klein, T. (2014) The variability of stomatal sensitivity to leaf water potential across tree species indicates a continuum between isohydric and anisohydric behaviours. *Functional Ecology*, 28, 1313–1320.

Klein, T. & Hartmann, H. (2018) Climate change drives tree mortality. *Science*, 362, 758.

Kursar, T.A., Engelbrecht, B.M.J., Burke, A., Tyree, M.T., El Omari, B. & Giraldo, J.P. (2009) Tolerance to low leaf water status of tropical tree seedlings is related to drought performance and distribution. *Functional Ecology*, 23, 93–102.

Lenth, R.V. 2022. emmeans: estimated Marginal Means, aka Least-Squares Means. R package version 1.7.2. https://CRAN.R-project.org/package=emmeans

Lesk, C., Rowhani, P. & Ramankutty, N. (2016) Influence of extreme weather disasters on global crop production. *Nature*, 529, 84–87.

Mantova, M., Herbette, S., Cochard, H. & Torres-Ruiz, J.M. (2022) Hydraulic failure and tree mortality: from correlation to causation. *Trends in Plant Science*, 27, 335–345.

Mantova, M., Menezes-Silva, P.E., Badel, E. & Cochard, H. (2021) The interplay of hydraulic failure and cell vitality explains tree capacity to recover from drought. *Physiologia Plantarum*, 172, 247–257.

Martinez-Vilalta, J., Anderegg, W.R., Sapes, G. & Sala, A. (2019) Greater focus on water pools may improve our ability to understand and anticipate drought-induced mortality in plants. *New Phytologist*, 223, 22–32.

Marusig, D., Petruzzellis, F., Tomasella, M., Napolitano, R., Altobelli, A. & Nardini, A. (2020) Correlation of field-measured and remotely sensed plant water status as a tool to monitor the risk of drought-induced forest decline. *Forests*, 11, 77.

McDowell, N., Allen, C.D., Anderson-Teixeira, K., Brando, P., Brienen, R., Chambers, J. et al. (2018) Drivers and mechanisms of tree mortality in moist tropical forests. *New Phytologist*, 219, 851–869.

McDowell, N.G., Brodribb, T.J. & Nardini, A. (2019) Hydraulics in the 21st century. *New Phytologist*, 224, 537–542.

McDowell, N.G., Pockman, W.T., Allen, C.D., Breshears, D.D., Cobb, N., Kolb, T. et al. (2008) Mechanisms of plant survival and mortality under drought: why do some plants survive while others succumb to drought? *New Phytologist*, 178, 719–739.

McDowell, N.G., Sapes, G., Pivovaroff, A., Adams, H.D., Allen, C.D., Anderegg, W.R.L. et al. (2022) Mechanisms of woody-plant mortality under rising drought, CO_2 and vapour pressure deficit, *Nature Reviews Earth & Environment*, 3, 294–308.

Mukarram, M., Choudhary, S., Kurjak, D., Anja Petek, A. & Khan, M.A. (2021) Drought: sensing, signalling, effects and tolerance in higher plants. *Physiologia Plantarum*, 172, 1291–130.

Nardini, A., Battistuzzo, M. & Savi, T. (2013) Shoot desiccation and hydraulic failure in temperate woody angiosperms during an extreme summer drought. *New Phytologist*, 200, 322–329.

Nardini, A., Petruzzellis, F., Marusig, D., Tomasella, M., Natale, S., Altobelli, A. et al. (2021) Water 'on the rocks': a summer drink for thirsty trees? *New Phytologist*, 229, 199–212.

Nardini, A., Savi, T., Trifilò, P. & Lo Gullo, M.A. (2018) Drought stress and the recovery from xylem embolism in woody plants. *Progress in Botany*, 79, 197–231.

Petruzzellis, F., Pagliarani, C., Savi, T., Losso, A., Cavalletto, S., Tromba, G. et al. (2018) The pitfalls of *in vivo* imaging techniques: evidence for cellular damage caused by synchrotron X-ray computed microtomography. *The New Phytologist*, 220, 104–110.

Pinheiro, J., Bates, D., Debroy, S. & Sarkar, D., R Core Team, 2016. Nlme nonlinear mixed effects models. R Package. Version 3.1-124.

Pokhrel, Y., Felfelani, F., Satoh, Y., Boulange, J., Burek, P., Gädeke, A. et al. (2021) Global terrestrial water storage and drought severity under climate change. *Nature Climate Change*, 11, 226–233.

Rao, K., Anderegg, W.R.L., Sala, A., Martnez-Vilalta, J. & Konings, A.G. (2019) Satellite-based vegetation optical depth as an indicator of drought-driven tree mortality. *Remote Sensing of Environment*, 227, 125–136.

Ritz, C., Baty, F., Streibig, J.C. & Gerhard, D. (2015) Dose-response analysis using R. *PLoS One*, 10, e0146021.
Ritz, C. & Streibig, J.C., 2009. Nonlinear regression in R. Springer.
Rodriguez-Dominguez, C.M. & Brodribb, T.J. (2020) Declining root water transport drives stomatal closure in olive under moderate water stress. *New Phytologist*, 225, 126–134.
Rosner, S., Heinze, B., Savi, T. & Dalla-Salda, G. (2019) Prediction of hydraulic conductivity loss from relative water loss: new insights into water storage of tree stems and branches. *Physiologia Plantarum*, 165, 843–854.
Saatchi, S., Asefi-Najafabady, S., Malhi, Y., Aragão, L.E.O.C., Anderson, L.O., Myneni, R.B. et al. (2013) Persistent effects of a severe drought on Amazonian forest canopy. *Proceedings of National Academy of Sciences of the United States of America*, 110, 565–570.
Sapes, G., Roskilly, B., Dobrowski, S., Maneta, M., Anderegg, W.R.L., Martinez-Vilalta, J. et al. (2019) Plant water content integrates hydraulics and carbon depletion to predict drought-induced seedling mortality. *Tree Physiology*, 39, 1300–1312.
Sapes, G. & Sala, A. (2021) Relative water content consistently predicts drought mortality risk in seedling populations with different morphology, physiology and times to death. *Plant, Cell & Environment*, 44, 3322–3335.
Savi, T., Marin, M., Luglio, J., Petruzzellis, F., Mayr, S. & Nardini, A. (2016) Leaf hydraulic vulnerability protects stem functionality under drought stress in *Salvia officinalis*. *Functional Plant Biology*, 43, 370–379.
Scoffoni, C., Chatelet, D.S., Pasquet-Kok, J., Rawls, M., Donoghue, M.J., Edwards, E.J. et al. (2016) Hydraulic basis for the evolution of photosynthetic productivity. *Nature Plants*, 2, 16072.
Skelton, R.P., Brodribb, T.J. & Choat, B. (2017) Casting light on xylem vulnerability in an herbaceous species reveals a lack of segmentation. *New Phytologist*, 214, 561–569.
Sperry, J.S. (2000) Hydraulic constraints on plant gas exchange. *Agricultural and Forest Meteorology*, 104, 13–23.
Tardieu, F., Draye, X. & Javaux, M. (2017) Root water uptake and ideotypes of the root system: whole-plant controls matter. *Vadose Zone Journal*, 16, 1–10.
Trifilò, P., Casolo, V., Raimondo, F., Petrussa, E., Boscutti, F., Lo Gullo, M.A. et al. (2017) Effects of prolonged drought on stem non-structural carbohydrates content and post-drought hydraulic recovery in *Laurus nobilis* L.: the possible link between carbon starvation and hydraulic failure. *Plant Physiology and Biochemistry*, 120, 232–241.
Trifilò, P., Nardini, A., Lo Gullo, M.A. & Salleo, S. (2003) Vein cavitation and stomatal behaviour of sunflower (*Helianthus annuus*) leaves under water limitation. *Physiologia Plantarum*, 119, 409–417.
Trifilò, P., Petruzzellis, F., Abate, E. & Nardini, A. (2021) The extra-vascular water pathway regulates dynamic leaf hydraulic decline and recovery in *Populus nigra*. *Physiologia Plantarum*, 172, 29–40.
Trueba, S., Pan, R., Scoffoni, C., John, G.P., Davis, S.D. & Sack, L. (2019) Thresholds for leaf damage due to dehydration: declines of hydraulic function, stomatal conductance and cellular integrity precede those for photochemistry. *New Phytologist*, 223, 134–149.
Tyree, M.T. & Hammel, H.T. (1972) The measurement of the turgor pressure and the water relations of plants by the pressure-bomb technique. *Journal of Experimental Botany*, 3, 267–282.
Tyree, M.T., Vargas, G., Engelbrecht, B.M.J. & Kursar, T.A. (2002) Drought until death do us part: a case study of the desiccation-tolerance of a tropical moist forest seedling-tree, (Hemsl.) Fritsch. *Journal of Experimental Botany*, 53, 2239–2247.
Urli, M., Porte, A.J., Cochard, H., Guengant, Y., Burlett, R. & Delzon, S. (2013) Xylem embolism threshold for catastrophic hydraulic failure in angiosperm trees. *Tree Physiology*, 33, 672–683.
Wang, X., Du, T., Huang, J., Peng, S. & Xiong, D. (2018) Leaf hydraulic vulnerability triggers the decline in stomatal and mesophyll conductance during drought in rice. *Journal of Experimental Botany*, 69, 4033–4045.
Xiong, D. & Nadal, M. (2020) Linking water relations and hydraulics with photosynthesis. *Plant Journal*, 101, 800–815.
Zhao, Z., Chen, G. & Zhang, C. (2001) Interaction between reactive oxygen species and nitric oxide in drought-induced abscisic acid synthesis in root tips of wheat seedlings. *Australian Journal of Plant Physiology*, 28, 1055–1061.

SUPPORTING INFORMATION

Additional supporting information can be found online in the Supporting Information section at the end of this article.

How to cite this article: Trifilò, P., Abate, E., Petruzzellis, F., Azzarà, M. & Nardini, A. (2023) Critical water contents at leaf, stem and root level leading to irreversible drought-induced damage in two woody and one herbaceous species. *Plant, Cell & Environment*, 46, 119–132. https://doi.org/10.1111/pce.14469